Energy

Volume 3, Issue 3, 284-296.
DOI: 10.3934/energy.2015.3.284
Received date 19 May 2015
Accepted date 15 July 2015
Published date 22 July 2015

http://www.aimspress.com/

Research article

Molten salt pyrolysis of milled beech wood using an electrostatic precipitator for oil collection

Heidi S. Nygård * and Espen Olsen

Department of Mathematical Sciences and Technology, Norwegian University of Life Sciences, 1430 Ås, Norway

*** Correspondence:** E-mail: heidi.nygard@nmbu.no; Tel: +47-67-23-15-72.

Abstract: A tubular electrostatic precipitator (ESP) was designed and tested for collection of pyrolysis oil in molten salt pyrolysis of milled beech wood (0.5–2 mm). The voltage-current (V-I) characteristics were studied, showing most stable performance of the ESP when N_2 was utilized as inert gas. The pyrolysis experiments were carried out in FLiNaK and $(LiNaK)_2CO_3$ over the temperature range of 450–600 °C. The highest yields of pyrolysis oil were achieved in FLiNaK, with a maximum of 34.2 wt% at 500 °C, followed by a decrease with increasing reactor temperature. The temperature had nearly no effect on the oil yield for pyrolysis in $(LiNaK)_2CO_3$ (19.0–22.5 wt%). Possible hydration reactions and formation of HF gas during FLiNaK pyrolysis were investigated by simulations (HSC Chemistry software) and measurements of the outlet gas (FTIR), but no significant amounts of HF were detected.

Keywords: beech wood; pyrolysis; molten salts; electrostatic; precipitator

1. Introduction

Pyrolysis is a thermochemical conversion process in which biomass is heated usually in the absence of oxygen. The products are pyrolysis oil, non-condensable gases and solid char, with respective yields depending on various process parameters such as heating rate, reaction temperature, and residence time in the hot zone of the reactor system [1]. In fast pyrolysis, the biomass particles should be heated rapidly to temperatures around 500 °C, followed by quenching of the produced vapors. In this way secondary reactions are kept to a minimum and the oil yield is maximized [2].

Inorganic molten salts are potential candidates for rapid heat transfer in fast pyrolysis due to their good heat transfer characteristics, thermal stability and large heat capacities [3]. However, there are limited reported results with focus on the yield of pyrolysis oil in molten salt pyrolysis. Jiang, et al. [4] performed an experimental study on pyrolysis of biomass in molten chlorides, and claimed that both the oil yield and water content of pyrolysis oil can be adjusted by varying the composition of the molten salt. The highest yield of pyrolysis oil (35.0 wt%) was obtained from cellulose pyrolysis in $ZnCl_2$ at 450 °C, while the use of other chloride mixtures ($ZnCl_2$-KCl, KCl-CuCl, $ZnCl_2$-KCl-CuCl, ZnCl-KCl-$FeCl_2$) gave yields up to 15.0 wt%. Other researchers have concentrated on gasification of cellulose in carbonates [5,6] or production of specific phenolic compounds from lignin in chlorides [7,8]. The use of molten salts have also been reported for thermal treatment of municipal refuse [9], wastepaper [10,11], and recycling of plastics [12,13,14]. Other applications of molten salts are as heat exchangers in solar power towers and nuclear power plants [15].

In most pyrolysis reactor configurations, a large volume of inert gas is needed for fluidization and/or transportation of the produced vapors out of the reactor [2]. This means that the vapors, which are mostly in the form of aerosols, are present at relatively low concentrations in an inert gas (< 5 vol%), and the separation is a difficult task [16,17]. Quenching by direct contact with product pyrolysis oil or in an immiscible hydrocarbon solvent has been widely practiced [1], but careful design and temperature control are needed to avoid blockages in the system due to a broad condensation temperature range of the organic volatiles [17]. Solvent methods have relatively high collection efficiencies, but the need for subsequent separation of the pyrolysis oil from the solvent adds cost to the process [18]. Lately, it has been more common to use electrostatic precipitation (ESP) [1]. In an ESP, the vapors are charged by a corona discharge and separated from the inert gas by an electric field. The charged droplets are attracted to a grounded wall where they are neutralized and collected [19]. This method has been found to be more effective than solvent and cooling methods for separation of pyrolysis vapors from the remaining gas stream [18]. However, the design and characteristics of the ESP are often left out of the publications.

There are two main objectives in the present paper. The first objective is the design of a tubular ESP for collection of pyrolysis oil. The voltage-current (V-I) characteristics are investigated with pure inert gases (N_2 and Ar) and with pyrolysis vapors included in the gas streams. The second objective is to use the ESP for collection of oil from molten salt pyrolysis of milled beech wood (0.5–2 mm). The choice of salts were selected based on previously reported heat transfer characteristics for thermal processing of biomass [20]. In a previous study [21], we found that molten FLiNaK gives significantly higher heating rates compared with a fluidized sand bed [22] for beech wood cylinders with $d \leq 4$ mm. In a subsequent study [23], both FLiNaK and $(LiNaK)_2CO_3$ showed good promise as heat transfer media in fast pyrolysis due to high heating rates for beech wood cylinders (d = 3.5 mm) in the temperature range of 450 to 600 °C.

In this study, we continue to use the most promising salts from our previous work as heat transfer media in molten salt pyrolysis. Pyrolysis experiments are performed in FLiNaK and $(LiNaK)_2CO_3$ in the temperature range 450–600 °C. The effects of salt mixture and reactor temperature on the yields of pyrolysis oil and char are investigated, and the oil is analyzed with respect to water content.

2. Materials and Method

2.1. Design characteristics of electrostatic precipitator

A schematic of the constructed ESP is shown in Figure 1, with the design adopted from Bedmutha et al. [19]. The inner cylinder was made of stainless steel and was electrically grounded. It was 50 mm in diameter and 150 mm long. A stainless steel wire (1 mm) co-axial with the inner cylinder was connected to a high voltage source and used as discharge electrode (positive potential). The outer cylinder was made of polyoxymethylene (POM), an insulating material with a low coefficient of friction, good dielectric properties and good resistance to oils, greases, and solvents [24]. The ESP was cooled externally with tap water (~7 °C).

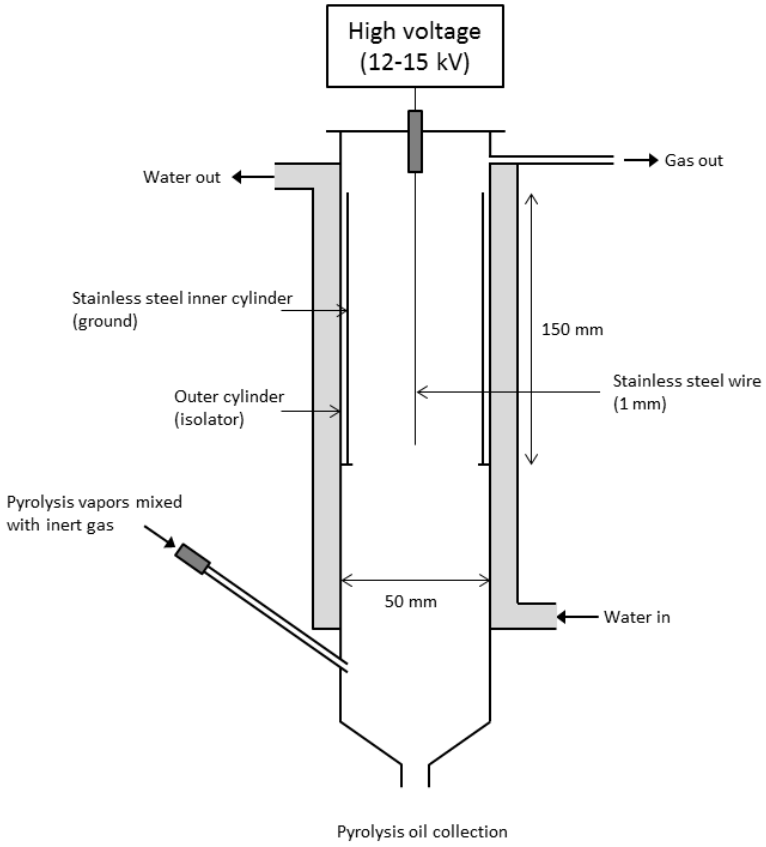

Figure 1. Schematic of the electrostatic precipitator (ESP).

For the initial testing, a bubble flask with water was attached at the exhaust of the ESP. It could be easily observed if the outlet gas contained any uncondensed pyrolysis vapors as these would fill the empty part of the flask with white "smoke". Argon (Ar, purity 99.99%, $H_2O \leq 20$ ppm, $O_2 \leq 20$ ppm) and nitrogen (N_2, purity 99.999%, $H_2O \leq 3$ ppm, $O_2 \leq 3$ ppm) obtained from AGA were used as inert gases.

The ESP was operated by setting the central electrode at a positive potential ranging from 0 to 20 kV, and the V-I characteristics (Figure 2) were determined with pure inert gases and during pyrolysis experiments with milled beech wood particles in FLiNaK at 500 °C. The voltage was increased slowly until spark-over occurred, and the values of the output voltage and current were

read directly from the power supply. The procedure was performed several times to assure reproducibility.

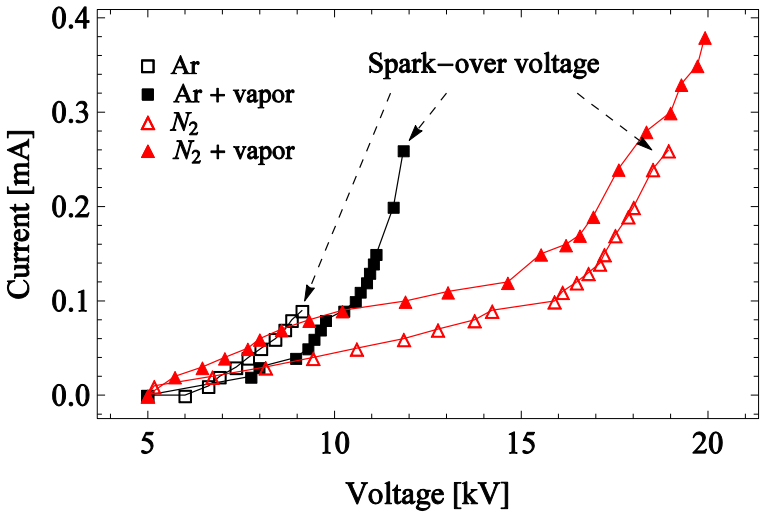

Figure 2. Current vs voltage characteristics for the electrostatic precipitator.

The two employed gases showed very different influence on the V-I characteristics, with the point for spark-over being the most prominent. Sparking is a phenomenon occurring when a conducting path is formed between the electrodes and electrons reach the grounded wall without being captured by molecules or particles. This can happen when the voltage is too high or the inert gas breaks down [25]. With pure inert gas streams, the spark-over occurred at 9.1 kV for Ar and 18.9kV for N_2. Argon and molecular nitrogen have similar ionization energies (1520.6 and 1503.0 kJ/mol, respectively [26]), but the break down voltages are generally observed to be lower for argon [27]. The different V-I behaviors could be caused by differences of impurities as well, an observation also reported by Bedmutha et al. [19]. In the presence of pyrolysis vapors, the spark-over voltage for Ar was increased to 11.9 kV, while no spark-over was observed for N_2 within the voltage range of the power supply. This could be explained by the pyrolysis vapors absorbing the electrons formed at the cathode and thus reducing the possibility for sparking.

It was visually observed that a minimum of 12 kV was required for separation of pyrolysis vapors and the remaining gas stream. Since these conditions were not possible without experiencing spark-overs using Ar, N_2 was chosen for the rest of the experiments in this study. Also, with N_2 as an inert gas, the increase in current with applied voltage is slower (Figure 2). This indicates poor conductivity of the gas, giving a more stable operation of the ESP.

2.2. Experimental procedure for pyrolysis of beech wood

Beech wood was used as feedstock in all the pyrolysis experiments. Beech wood is a hardwood consisting of 48% cellulose, 28% hemicellulose, 22% lignin and 2% extractives [28]. Untreated beech wood logs were milled and sieved, and a fraction of particle diameter of 0.5–2 mm was used. The samples were dried at 105 °C for 24 h prior to the experiments in order to minimize the water content.

The salts were obtained separately in their simplest form from Sigma-Aldrich (> 98.5% purity). The salt mixtures as listed in Table 1 were prepared by direct mixing of the pure compounds before every experiment by means of weighing. The mixtures were pre-melted at 500 °C and kept in a drying cabinet (> 200 °C) for at least 24 h.

Table 1. Composition and properties of salts used in the experiments.

Molten salts composition (wt%)	Melting point	Experiment temperatures
LiF-NaF-KF (29.2-11.7-59.1)	454 ℃ [15]	475–600 °C
Li_2CO_3-Na_2CO_3-K_2CO_3 (31.7-33.7-34.7)	397 °C[29]	450–600 °C

300 g of dried salt mixture was filled in a nickel crucible (H = 190 mm, ID = 52 mm) placed inside a stainless steel reactor (H = 200 mm, ID = 62 mm) that was heated externally by a tubular electric furnace (Figure 3). Nickel was chosen because it is more resistant to corrosion by molten salts [30]. The height of the melt varied between 60 and 70 mm, depending on the type of salt mixture and reactor temperature.

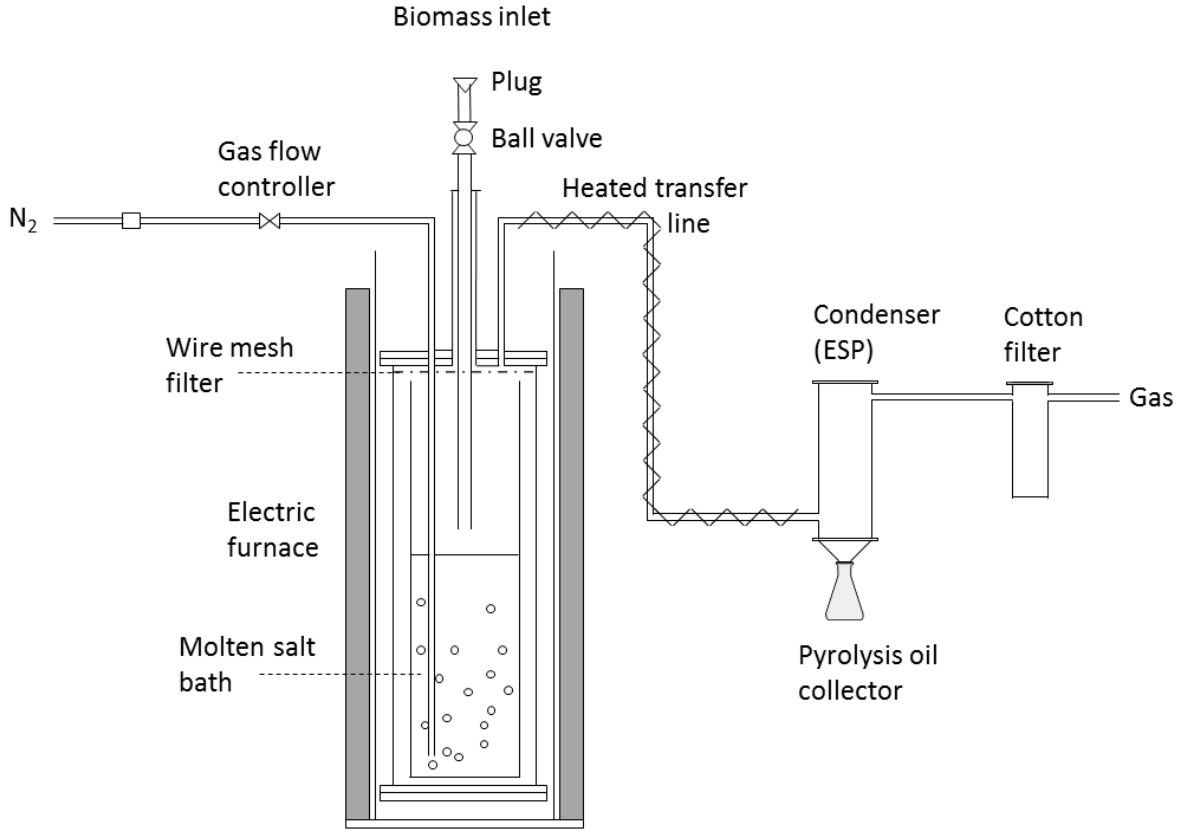

Figure 3. Schematic representation of the experimental setup for pyrolysis of biomass in molten salts.

A 9 μm wire mesh filter was placed at the exit of the reactor to remove char and ash from the hot pyrolysis vapors. This type of in situ vapor filtration prior to condensation has been shown to

give yields comparable to those obtained when cyclones are used, but with less solids, alkali metals, and ash in the pyrolysis oil [31]. The filter also ensures that possibly unreacted wood particles remain in the hot reactor.

When the heating was started, inert gas (N_2) was continuously flowed into the reactor through a nickel tube (4 mm) to ensure an oxygen-free atmosphere. The salt temperature was monitored by a submerged type K thermocouple. Once the salt was completely melted, the nickel tube was submerged in the melt to give turbulent mixing and a homogeneous temperature throughout the reactor. Turbulent mixing enhances the heat transfer from the salt to the wood samples in the pyrolysis process. The heating was continued until the desired reactor temperature was reached. The temperature ranges used in the experiments for the two salt compositions are listed in Table 1.

The samples were introduced to the reactor manually through a ball valve based feeding system. The small particles were filled in a tube above the ball valve. The tube was then closed with a plug, and the valve was opened to feed the wood to the reactor. No gas could escape to the environment in this closed system. Due to problems with clogging of the feeding tube, the tube was kept 1–2 cm above the molten salt bath and the particles were fed to the top of the melt with the aid of a push rod. A total of 20–25 grams was added in small batches of 0.3–0.5 gram every minute. In preliminary experiments, the mixing of wood particles with a fluid bed (water-sugar solution to obtain similar characteristics as molten salts) was studied visually in a cold-flow glass model. At room temperature, the particles were mixed well in the fluid due to the turbulent bubbling of inert gas.

The flow rate of N_2 was set to 0.6 L/min during the experiments. This was a tradeoff between relatively short vapor residence time in the order of a few seconds and to avoid extensive splashing of the salt which could possibly clog the wire mesh filter at the top of the reactor. The vapors were led out of the reactor through a 4 mm heated transfer line (450 °C) made of stainless steel. The system was connected to the previously described ESP for collection of pyrolysis oil. The ESP was operated at 12–15 kV and cooled externally with tap water at 7 °C. A tubular cotton gas filter (filtration level 10 μm) was attached to the exhaust of the ESP for capturing the remaining vapors, and the non-condensable gases were vented off. After the experiments were completed, the power was turned off, and the system was left under inert atmosphere until ambient temperature to prevent corrosion.

The char yield was measured as difference between the reactor mass before and after experiment. The total pyrolysis oil yield was determined by weighing the ESP condenser and the cotton filter before and after the experiment. The water content of the oil was determined by Karl Fischer titration, using Hydranal Composite 5 as titer.

3. Results and Discussion

Three identical experiments with beech wood in FLiNaK at 500 °C were conducted to assure reproducibility of the experimental method. The remaining experiments were performed once. For the successful experiments, no uncondensed pyrolysis vapors were observed at the outlet of the condenser system consisting of the ESP and the cotton filter. The ESP contained between 92 and 97% of the produced pyrolysis oil, with the remaining amount found in the cotton filter. Only the fraction condensed in the ESP was analyzed further with respect to water content. The collected oil was in one phase in the case of FLiNaK at 475 and 500 °C, while a two-phase oil was recovered for the rest

of the experiments. The two-phase samples were heated slowly until good mixing was achieved before the water content was determined.

3.1. Effect of salt mixture and temperature on product yields

The yields of pyrolysis oil and solid char as a function of reactor temperature are plotted in Figure 4. Figure 5 shows the influence of reactor temperature and salt composition on the water content of the pyrolysis oil.

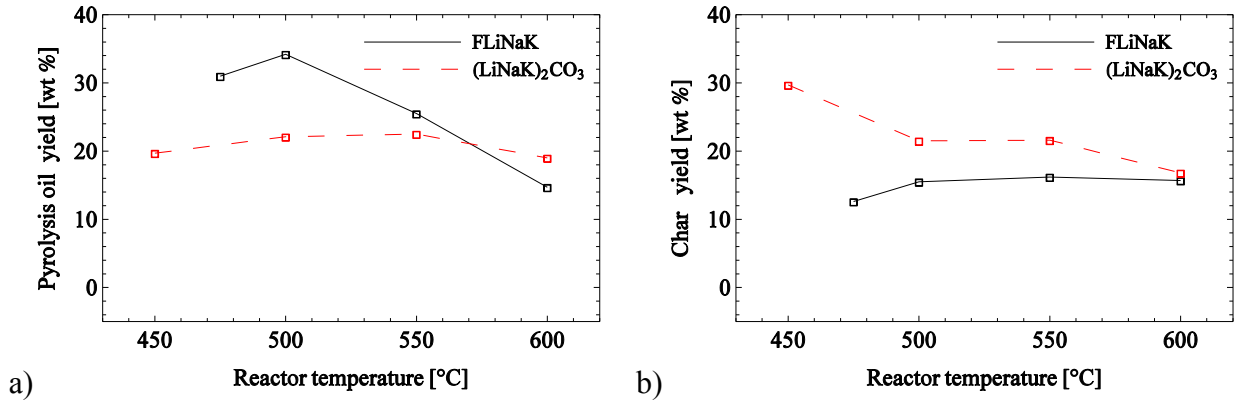

Figure 4. Yields of pyrolysis oil (a) and solid char (b) as function of the reactor temperature in FLiNaK (black) and $(LiNaK)_2CO_3$ (red).

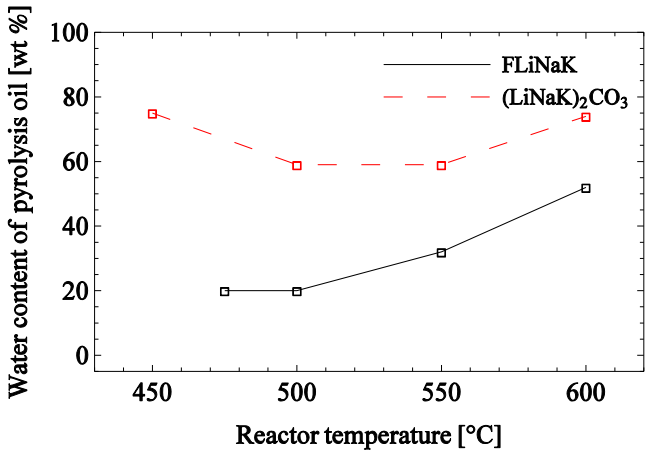

Figure 5. Water content of pyrolysis oil (collected from the ESP) as a function of reactor temperature for pyrolysis of beech wood in FLiNaK (black) and $(LiNaK)_2CO_3$ (red).

The reactor temperature showed a strong effect on the pyrolysis oil yield in FLiNaK, with a maximum of 34.2 wt% at 500 °C, followed by a decrease with increasing reactor temperature. The yield of pyrolysis oil in $(LiNaK)_2CO_3$ was nearly constant with temperature, with values between 19.0 and 22.5 wt%. For the char yield, only a minor temperature dependence was observed in both

salt mixtures for reactor temperatures above 500 °C. The water content varied greatly between pyrolysis in FLiNaK and $(LiNaK)_2CO_3$, but the same trend with lower water content for higher oil yields are observed.

According to the Broido-Shafizadeh model, pyrolysis starts with an intermediate pre-reaction in which an active substance is formed [32]. The formation of a liquid intermediate has been experimentally confirmed both for pyrolysis of cellulose [33,34] and lignin [35], the main constituents of lignocellulosic biomass. This pre-reaction is followed by two competing first-order reactions: dehydration and depolymerization. Dehydration is usually associated with lower heating rates and lower temperatures (< 300 °C), and the primary products are char, water and CO_2. Depolymerization is favored for faster heating rates and higher temperatures, and the primary products are vapors that may condense as pyrolysis oil [32]. If the molecules cannot escape from the primary products, secondary reactions will occur, leading to secondary char, oils, and gases [35]. These reactions could be intra- or extra-particle reactions, and they could occur either homogeneously in the vapor phase or heterogeneously by reaction with formed char or unreacted wood [36]. The liquid intermediate from the pre-reaction is also found to be a reactive medium for reactions such as dehydration and cross-linking [37]. The rate of volatiles mass transport within and away from the particle will influence the extent of the secondary reactions [36].

In this study, the pyrolysis oil yields are for the most part higher than those reported in molten chloride pyrolysis by Jiang et al. [4], where cold trap condensers were utilized for oil collection. This indicates that the use of ESP is a better solution for separation of pyrolysis oils from the remaining gas stream in molten salt pyrolysis. On the other hand, the oil yields are generally lower and the char yields higher compared to typical values reported for other fast pyrolysis technologies [2]. These results, in addition to the high water contents of the pyrolysis oils (Figure 5), point towards the occurrence of secondary reactions. In our previous studies [21,23], we have confirmed high heating rates for single beech wood particles in FLiNaK and $(LiNaK)_2CO_3$, indicating that depolymerization towards condensable vapors should be the dominant pathway. It was also confirmed experimentally that the reaction temperatures were in the range of fast pyrolysis conditions rather than slow pyrolysis (carbonization) conditions. Secondary cracking inside the particles should also be unimportant in the present study due to the small particles involved [2].

Extra-particle reactions could on the other hand occur if the primary products are not able to escape from the hot reactor, resulting in the formation of secondary char, non-condensable gases and water. Even though the inert gas should bring the vapors out of the reactor within a few seconds, the vapors could experience mass transfer resistance in the melt leading to longer vapor residence time at elevated temperatures. However, several researchers have stated that the oil yield is much less dependent on vapor residence times than originally assumed. Wang et al. [38] did not observe any effect on the product yields for vapor residence times between 1 and 6 seconds, while Scott et al. [39] found no significant influence up to 10 seconds. Hoekstra et al. [40] stated that pyrolysis vapors can be exposed to elevated temperatures for a long time, given that these are poor in mineral content, since minerals containing alkali elements such as Na and K promote the formation of gaseous species and char on the expense of pyrolysis oil. Taking this into account, we propose that the presence of minerals in the molten salts play an important role in the pyrolysis process, and that the lower yields of pyrolysis oil are caused by a combination of longer vapor residence times and prolonged contact between the salts and the formed vapors.

Another possible explanation is insufficient mixing of wood and salt leading to slower heating than assumed based on our previous work [21,23], and thus dehydration and carbonization reactions could take place at lower temperatures on the expense of depolymerization to condensable gases. This could explain the high water contents observed. However, turbulent bubbling and splashing of the molten salt should ensure the same contact between the hot melt and the wood particles giving heating rates typical for fast pyrolysis. Nevertheless, for further studies, the reactor setup should be redesigned to enhance the mixing of milled wood and molten salt by mechanical stirring in addition to inert gas bubbling. Continuously feeding of the feedstock by e.g. a mechanical screw would also give smoother feeding and ensure better mixing.

3.2. *Possible formation of HF in FLiNaK pyrolysis*

Hydration of metal halides can result in formation of HX, where X represents a halide ion. Given the hygroscopic nature of FLiNaK, formation of HF gas (Eqs. 1–6) is a possible concern when this salt is utilized in pyrolysis where water is one of the species formed in the process. The HF gas could contaminate the pyrolysis products and also lead to extensive corrosion of metal elements found in process equipment [41].

$$2LiF(l) + H_2O(g) \leftrightarrow Li_2O(l) + 2HF(g) \quad (1)$$

$$2NaF(l) + H_2O(g) \leftrightarrow Na_2O(l) + 2HF(g) \quad (2)$$

$$2KF(l) + H_2O(g) \leftrightarrow K_2O(l) + 2HF(g) \quad (3)$$

$$LiF(l) + H_2O(g) \leftrightarrow LiOH(l) + HF(g) \quad (4)$$

$$NaF(l) + H_2O(g) \leftrightarrow NaOH(l) + HF(g) \quad (5)$$

$$KF(l) + H_2O(g) \leftrightarrow KOH(l) + HF(g) \quad (6)$$

The hydration reactions were simulated in HSC Chemistry software [42]. This is a chemical reaction and equilibrium software with extensive thermochemical database and flowsheet simulation. We have used the software to calculate Gibbs free energy as a function of temperature for each reaction, with the results plotted in Figure 6. According to the simulations, hydration will not occur for FLiNaK pyrolysis due to positive Gibbs free energies in the experimental temperature ranges of this study. It should be noted that the Gibbs free energies are well above zero for temperatures relevant for gasification processes as well.

The modeling results were verified experimentally by analyzing the outlet gas by means of a FTIR gas analyzer (Thermo Scientific, Nicolet 6700). No significant amounts of HF were detected during pyrolysis of milled beech wood in FLiNaK.

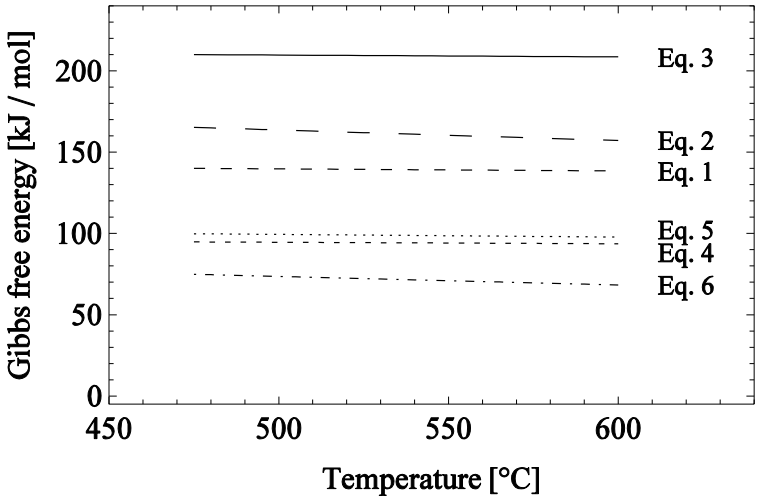

Figure 6. Gibbs free energy versus temperature for possible hydration reactions in FLiNaK.

4. Conclusion

The aim of this work was to design and test an electrostatic precipitator (ESP) for oil collection in molten salt pyrolysis of milled beech wood. The voltage-current (V-I) characteristics of the ESP were studied with the inert gases N_2 and Ar, and N_2 was found to give the most stable operation. This was attributed to higher break down voltages, lower concentrations of impurities, and lower conductivity of the inert gas. The minimum voltage required for separation of pyrolysis vapors from the remaining gas stream was found to be 12 kV.

Beech wood particles (0.5–2 mm) were pyrolyzed in FLiNaK and $(LiNaK)_2CO_3$ at temperatures between 450 and 600 °C. The ESP worked well, and no uncondensed vapors were observed at the gas outlet. The pyrolysis oil yields were generally higher than those reported in chloride pyrolysis by Jiang et al. [4], with a maximum of 34.2 wt% for FLiNaK at 500 °C. The pyrolysis oil yields were lower and the char yields higher compared to other fast pyrolysis technologies. The oils were also high in water content. These results were somewhat unexpected, since the employed molten salts have been found to give very high heating rates and typical fast pyrolysis reaction temperatures for beech wood particles in our previous work [21,23]. We propose that the main reason for this is a combination of mass transfer resistance leading to longer vapor residence times at elevated temperatures and at the same time giving prolonged contact with alkali elements (Na/K) found in the melts catalyzing extra-particle secondary reactions into char, non-condensable gases and water.

A possible concern when using FLiNaK as a reaction medium in thermochemical conversion of biomass is the reaction between the salt and produced water to form HF gas. According to both simulations and FTIR measurements of the outlet gas, no significant amounts of HF are produced during beech wood pyrolysis in FLiNaK.

Conflict of Interest

All authors declare no conflicts of interest in this paper.

References

1. Bridgwater AV (2012) Review of fast pyrolysis of biomass and product upgrading. *Biomass Bioenerg* 38: 68–94.
2. Venderbosch RH, Prins W (2010) Fast pyrolysis technology development. *Biofuel Bioprod Bior* 4: 178–208.
3. Lovering DG (1982) *Molten salt technology*. California, USA: Plenum Press. 533.
4. Jiang H, Ai N, Wang M, et al. (2009) Experimental Study on Thermal Pyrolysis of Biomass in Molten Salt Media. *Electrochemistry* 77: 730–735.
5. Adinberg R, Epstein M, Karni J (2004) Solar Gasification of Biomass: A Molten Salt Pyrolysis Study. *J Sol Energ Eng* 126: 850–857.
6. Hathaway BJ, Davidson JH, Kittelson DB (2011) Solar Gasification of Biomass: Kinetics of Pyrolysis and Steam Gasification in Molten Salt. *J Sol Energ Eng* 133: 021011.
7. Sada E, Kumazawa H, Kudsy M (1992) Pyrolysis of lignins in molten salt media. *Ind Eng Chem Res* 31: 612–616.
8. Kudsy M, Kumazawa H, Sada E (1995) Pyrolysis of kraft lignin in molten ZNCL2-KCL media with tetralin vapor addition. *Can J Chem Eng* 73: 411–415.
9. Hammond V, Mudge L (1975) Feasibility study of use of molten salt technology for pyrolysis of solid waste. Richland, Washington, USA: Battele Pacific Northwest Labs. EPA-670/2-75-014 EPA-670/2-75-014.
10. Iwaki H, Ye S, Katagiri H, et al. (2004) Wastepaper gasification with CO2 or steam using catalysts of molten carbonates. *Appl Catal A: Gen* 270: 237–243.
11. Jin G, Iwaki H, Arai N, et al. (2005) Study on the gasification of wastepaper/carbon dioxide catalyzed by molten carbonate salts. *Energy* 30: 1192–1203.
12. Menzel J, Perkow H, Sinn H (1973) Recycling plastics. *Chem Ind* 570–573.
13. Bertolini GE, Fontaine J (1987) Value recovery from plastics waste by pyrolysis in molten salts. *Conserv Recy* 10: 331–343.
14. Chambers C, Larsen JW, Li W, et al. (1984) Polymer waste reclamation by pyrolysis in molten salts. *Ind Eng Chem Proc Des Dev* 23: 648–654.
15. Williams D (2006) Assessment of candidate molten salt coolants for the NGNP/NHI heat-transfer loop. Oak Ridge, Tennessee, USA: Oak Ridge National Laboratory.
16. Bridgwater AV, Peacocke GVC (2000) Fast pyrolysis processes for biomass. *Renew Sust Energ Rev* 4: 1–73.
17. Oasmaa A, Peacocke C (2010) Properties and fuel use of biomass-derived fast pyrolysis liquids. VTT Publications: Finland 731: 79.
18. Mochizuki T, Toba M, Yoshimura Y (2013) Effect of Electrostatic Precipitator on COllection Efficiency of Bio-oil in Fast Pyrolysis of Biomass. *J Jpn Petrol Inst* 56: 401–405.
19. Bedmutha RJ, Ferrante L, Briens C, et al. (2009) Single and two-stage electrostatic demisters for biomass pyrolysis application. *Chem Eng Proc: Proc Intens* 48: 1112–1120.

20. Nygård HS, Olsen E (2012) Review of thermal processing of biomass and waste in molten salts for production of renewable fuels and chemicals. *Int J Low-Carbon Technol*: ctr045.
21. Nygård HS, Danielsen F, Olsen E (2012) Thermal History of Wood Particles in Molten Salt Pyrolysis. *Energ Fuels* 26: 6419–6425.
22. Di Blasi C, Branca C (2003) Temperatures of Wood Particles in a Hot Sand Bed Fluidized by Nitrogen. *Energ Fuels* 17: 247–254.
23. Nygård HS, Olsen E (2014) Effect of Salt Composition and Temperature on the Thermal Behavior of Beech Wood in Molten Salt Pyrolysis. *Energ Procedia* 58: 221–228.
24. Lüftl S, Visakh P, Chandran S (2014) *Polyoxymethylene Handbook: Structure, Properties, Applications and Their Nanocomposites*. New Jersey, USA: John Wiley & Sons.
25. Lucas JR (2001) High voltage engineering. *Colombo, Open University of Sri Lanka* 64-89.
26. Huheey JE, Keiter EA, Keiter RL, et al. (2006) *Inorganic Chemistry: Principles of Structure and Reactivity*. Delhi, India: Pearson Education, 808.
27. Klas M, Radmilović-Radjenović M, Radjenović B, et al. (2012) Transport parameters and breakdown voltage characteristics of the dry air and its constituents. *Nucl Instrum Meth B:* 279: 96–99.
28. Grønli MG (1996) A theoretical and experimental study of the thermal degradation of biomass [Doctoral thesis]. Trondheim, Norway: The Norwegian University of Science and Technology. 282 .
29. Hathaway BJ, Davidson JH, Kittelson DB (2011) Solar Gasification of Biomass: Kinetics of Pyrolysis and Steam Gasification in Molten Salt. *J Sol Energ Eng* 133: 021011–021011.
30. Olson LC, Ambrosek JW, Sridharan K, et al. (2009) Materials corrosion in molten LiF–NaF–KF salt. *J Fluorine Chem* 130: 67–73.
31. Hoekstra E, Hogendoorn KJ, Wang X, et al. (2009) Fast pyrolysis of biomass in a fluidized bed reactor: in situ filtering of the vapors. *Ind Eng Chem Res* 48: 4744–4756.
32. Basu P (2013) *Biomass Gasification, Pyrolysis and Torrefaction: Practical Design and Theory*. San Diego, USA: Elsevier Science 552.
33. Kersten S, Garcia-Perez M (2013) Recent developments in fast pyrolysis of ligno-cellulosic materials. *Curr Opin Biotech* 24: 414–420.
34. Wang Z, McDonald AG, Westerhof RJ, et al. (2013) Effect of cellulose crystallinity on the formation of a liquid intermediate and on product distribution during pyrolysis. *J Anal Appl Pyrol* 100: 56–66.
35. Zhou S, Pecha B, van Kuppevelt M, et al. (2014) Slow and fast pyrolysis of Douglas-fir lignin: Importance of liquid-intermediate formation on the distribution of products. *Biomass Bioenerg* 66: 398–409.
36. Boroson ML (1987) Secondary reactions of tars from pyrolysis of sweet gum hardwood [Doctoral thesis]: Massachusetts Institute of Technology.
37. Dauenhauer PJ, Colby JL, Balonek CM, et al. (2009) Reactive boiling of cellulose for integrated catalysis through an intermediate liquid. *Green Chem* 11: 1555–1561.
38. Wang X, Kersten SRA, Prins W, et al. (2005) Biomass Pyrolysis in a Fluidized Bed Reactor. Part 2: Experimental Validation of Model Results. *Ind Eng Chem Res* 44: 8786–8795.
39. Scott DS, Majerski P, Piskorz J, et al. (1999) A second look at fast pyrolysis of biomass—the RTI process. *J Anal Appl Pyrol* 51: 23–37.

40. Hoekstra E, Westerhof RJM, Brilman W, et al. (2012) Heterogeneous and homogeneous reactions of pyrolysis vapors from pine wood. *AIChE J* 58: 2830–2842.
41. Ouyang F-Y, Chang C-H, Kai J-J (2014) Long-term corrosion behaviors of Hastelloy-N and Hastelloy-B3 in moisture-containing molten FLiNaK salt environments. *J Nucl Mater* 446: 81–89.
42. Roine A, Lamberg P, Mansikka-aho J, et al. (2006) HSC Chemistry 6.12. Helsinki, Finland: Outotec Research Oy.

AIMS Press